

Implementation of the Gamma Gaussian Inverse Wishart Trajectory Probability Hypothesis Density Filter

Jakob Sjudin, Martin Marcusson *SafeRadar Research Sweden*
Gothenburg, Sweden
firstname.lastname@saferadar.se

CONTENTS

I Introduction

I-A	Notation	
I-B	The τ operator	

II Prediction

III Update

IV Trajectory extraction

V Extension Smoothing

VI Mixture Reduction

VII Results

VII-A	Scenario 1	
VII-B	Scenario 2	

ABSTRACT

This report contains equations used in the Gamma Gaussian inverse Wishart trajectory probability hypothesis density (GGIWT-PHD) filter. It also contains results from two different scenarios where the GGIWTPHD filter is compared with the Gamma Gaussian inverse Wishart trajectory probability hypothesis density (GGIWPHD) filter. **Keywords:** Multiple object tracking, Extended objects, Gamma Gaussian inverse Wishart, Trajectories, Sensor fusion, Bayesian smoothing, Random finite sets, PHD filtering.

I. INTRODUCTION

This technical report contains equations for the filter recursions of the GGIWTPHD filter. The filter operates by the steps outlined in Fig. I.1.

Note that this report is a supplementary resource to the paper titled *Extended Object Tracking Using Sets Of Trajectories with a PHD Filter*. To fully understand the notation and equations presented here, it is advised to have the aforementioned paper at hand.

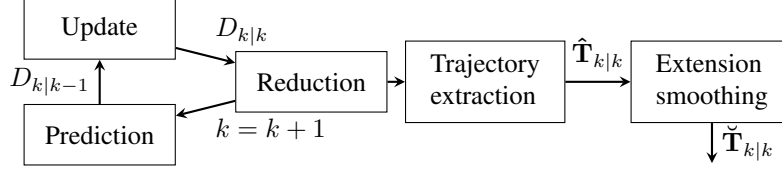


Fig. I.1: Flowchart of the GGIWTPHD filter recursion.

A. Notation

The $\mathcal{GGIW}\mathcal{T}$ mixture made up of a sum of weighted mixture components:

$$D_k = \sum_{j=1}^{J_k} w_k \mathcal{GGIW}\mathcal{T} \left(\mathcal{T}_k^{(j)}; \zeta_k^{(j)} \right) \quad (1)$$

Where ζ_k represents the GGIWT mixture parameters:

$$\zeta_k^{(j)} = \left\{ \alpha_k^{(j)}, \beta_k^{(j)}, m_k^{n,(j)}, P_k^{n,(j)}, v_k^{n,(j)}, V_k^{n,(j)} \right\} \quad (2)$$

Where

- α_k, β_k denote the shape and rate parameters of the gamma distribution at time k .
- v_k^n, V_k^n denote the trajectories of the degrees of freedom and scale matrix of the Inverse Wishart Distribution from the birth of the trajectory $t^{(j)}$ up until timestep $k = n^{(j)} - t^{(j)}$.
- m_k^n, P_k^n denote the trajectory of the mean and covariance of the normal distribution from the birth of the trajectory up until timestep $k = n^{(j)} - t^{(j)}$.

B. The τ operator

When working with trajectories, it is often of interest to only consider the most recent addition to the trajectory. This is done by defining the $\tau_k(\cdot)$ operator. Given a set of trajectories \mathbf{T} , the set $\tau_k(\mathbf{T})$ of target states at time k is

$$\tau_k(\mathbf{T}) = \bigcup_{\mathcal{T} \in \mathbf{T}} \tau_k(\mathcal{T}) \quad (3)$$

Where $\tau_k(\mathcal{T})$ picks out the most recent parameters m, P, V and v in the trajectory.

II. PREDICTION

The predicted PHD consists of two parts, one for new objects that appear in the surveillance area (birth) and one for objects that stay in the surveillance area from previous time steps (survive). This PHD is represented by a GGIWT mixture and is defined as

$$D_{k+1|k}(\mathcal{T}_{k+1}) = D_{k+1}^b(\mathcal{T}_{k+1}) + D_{k+1|k}^s(\mathcal{T}_{k+1}) \quad (4)$$

where $D_k^b(\mathcal{T}_k)$ is the birth intensity and $D_{k+1|k}^s(\mathcal{T}_{k+1})$ is the intensity for surviving existing targets which is defined as

$$D_{k+1|k}^s(\mathcal{T}_{k+1}) = \sum_{j=1}^{J_{k|k}} w_{k+1|k}^{(j)} \mathcal{GGIW}\mathcal{T} \left(\mathcal{T}_{k+1}; \zeta_{k+1|k}^{(j)} \right) \quad (5)$$

Objects that stay in surveillance area are modeled by the probability of survival P_S , which yields the weight update

$$w_{k+1|k}^{(j)} = P_S w_{k|k}^{(j)} \quad (6)$$

The details for the prediction step is given in Table I.

TABLE I: Equations for the GGIWTPHD filter prediction step

$$\begin{aligned}
w_{k+1|k}^{(j)} &= P_S w_{k|k}^{(j)} \\
\alpha_{k+1|k}^{(j)} &= \frac{\alpha_{k|k}^{(j)}}{\eta_k}, \quad \beta_{k+1|k}^{(j)} = \frac{\beta_{k|k}^{(j)}}{\eta_k} \\
m_{k+1|k}^{n,(j)} &= \left[(m_{k+1|k}^{n-1,(j)})^\top, \quad (\dot{F}^{(j)} m_{k+1|k}^{n-1,(j)})^\top \right]^\top \\
P_{k+1|k}^{n,(j)} &= \begin{bmatrix} P_{k|k}^{n-1,(j)} & P_{k|k}^{n-1,(j)} (\dot{F}_{k+1|k}^{(j)})^\top \\ \dot{F}_{k+1|k}^{(j)} P_{k|k}^{n-1,(j)} & \dot{F}_{k+1|k}^{(j)} P_{k|k}^{n-1,(j)} (\dot{F}_{k+1|k}^{(j)})^\top + Q \end{bmatrix} \\
v_{k+1|k}^{(j)} &= d + 1 + \psi^{-1} (v_{k|k}^{(j)} - d - 1), \quad v_{k+1|k}^{n,(j)} = \begin{bmatrix} v_{k|k}^{n-1,(j)} & v_{k|k}^{(j)} \end{bmatrix} \\
V_{k+1|k}^{(j)} &= \psi^{-1} \left(1 - \frac{d+1}{s} \right) \left(1 - \frac{d+1}{s} \right) C_2, \quad V_{k+1|k}^{n,(j)} = \begin{bmatrix} V_{k|k}^{n-1,(j)} & V_{k|k}^{(j)} \end{bmatrix} \\
\psi &= 1 + (v_{k|k}^{(j)} - 2d - 2) \left(\frac{1}{s} + \frac{1}{n} + \frac{d+1}{ns} \right) \\
s &= \frac{d+1}{d} \text{Tr} \{ C_1 C_2 (C_1 C_2 - \mathbf{I}_d)^{-1} \} \\
F^{(j)} &= \mathbf{J}_{\mathbf{f}_k}(\mathbf{x})|_{\mathbf{x}=\tau(m_{k|k}^{n-1,(j)})} \\
C_1 &= \mathbb{E}_{k|k} \left[\left(M_x \tau(V_{k|k}^{n-1,(j)}) M_x^\top \right)^{-1} \right], \quad C_2 = \mathbb{E}_{k|k} \left[M_x \tau(V_{k|k}^{n-1,(j)}) M_x^\top \right] \\
\dot{F}_{k+1|k}^{(j)} &= [0_{1,n-1}, \quad 1] \otimes F^{(j)}(\tau(m_{k|k}^{n-1,(j)}))
\end{aligned}$$

Where

- P_s denotes the probability of survival
- η_k denotes the measurement rate uncertainty
- d denotes the number of rows/columns in V
- M_x denotes a state-dependent matrix, typically a rotation matrix that depends on the objects turn-rate
- C_1 and C_2 are approximated using a third-order Taylor expansion as in [1]

III. UPDATE

For each cell \mathbf{W} in each partition \mathcal{P} the centroid measurement and scatter matrix are defined as

$$\bar{\mathbf{z}}_k^{\mathbf{W}} = \frac{1}{|\mathbf{W}|} \sum_{\mathbf{z}_k^{(i)} \in \mathbf{W}} \mathbf{z}_k^{(i)} \quad (7)$$

$$\mathbf{Z}_k^{\mathbf{W}} = \sum_{\mathbf{z}_k^{(i)} \in \mathbf{W}} (\mathbf{z}_k^{(i)} - \bar{\mathbf{z}}_k^{\mathbf{W}})(\mathbf{z}_k^{(i)} - \bar{\mathbf{z}}_k^{\mathbf{W}})^{\top} \quad (8)$$

With a predicted PHD intensity, the next step is a measurement update and calculation of a posterior PHD which is defined as

$$D_{k|k}(\mathcal{T}_k) = D_{k|k}^m(\mathcal{T}_k) + D_{k|k}^b(\mathcal{T}_k) + D_{k|k}^d(\mathcal{T}_k) \quad (9)$$

This consists of three parts, $D_{k|k}^m$ which represents not detected previously existing objects, $D_{k|k}^b$ which represents new targets appearing at measurement cluster centers and finally $D_{k|k}^d$ which represents detected previously existing targets. $D_{k|k}^d$ is updated according to the measurement model.

The GGIWT mixture for new object births:

$$D_{k|k}^b(\mathcal{T}_k) = \sum_{\mathcal{P} \angle \mathbf{Z}_k} \sum_{\mathbf{W} \in \mathcal{P}} w_{k|k}^{(b, \mathbf{W})} \mathcal{GGIWT}(\mathcal{T}_k; \zeta_{k|k}^{(b, \mathbf{W})}) \quad (10)$$

And the GGIWT mixture for previously detected objects:

$$D_{k|k}^d(\mathcal{T}_k) = \sum_{\mathcal{P} \angle \mathbf{Z}_k} \sum_{\mathbf{W} \in \mathcal{P}} \sum_{j=1}^{J_{k|k}-1} w_{k|k}^{(j, \mathbf{W})} \mathcal{GGIWT}(\mathcal{T}_k; \zeta_{k|k}^{(j, \mathbf{W})}) \quad (11)$$

And the GGIWT mixture for not detected, previously existing objects:

$$D_{k|k}^m(\mathcal{T}_k) \approx \sum_{j=1}^{J_{k|k}-1} \tilde{w}_{k|k}^{(j)} \mathcal{GGIWT}(\mathcal{T}_k; \tilde{\zeta}_{k|k}^{(j)}) \quad (12)$$

Where $\tilde{\zeta}_{k|k}^{(j)} = \left\{ \tilde{\alpha}_{k|k}^{(j)}, \tilde{\beta}_{k|k}^{(j)}, m_{k|k-1}^{n, (j)}, P_{k|k-1}^{n, (j)}, v_{k|k-1}^{n, (j)}, V_{k|k-1}^{n, (j)} \right\}$ where $\tilde{w}_{k|k}^{(j)}$, $\tilde{\alpha}_{k|k}^{(j)}$ and $\tilde{\beta}_{k|k}^{(j)}$ are obtained using a gamma-mixture reduction[2][3].

TABLE II: Equations for the GGIWTPHD filter update step

New objects

$$\alpha_{k|k}^{(b, \mathbf{W})} = \alpha_k^{(b)} + |\mathbf{W}|, \quad \beta_{k|k}^{(b, \mathbf{W})} = \beta_k^{(b)} + 1$$

$$m_{k|k}^{(b, \mathbf{W})} = \left[\left(\hat{\mathbf{z}}_k^{(b, \mathbf{W})} \right)^\top, \left(m_k^{(b)} \right)^\top \right]^\top, \quad P_{k|k}^{(b, \mathbf{W})} = \text{blkdiag} \left(Z_k^{(b, \mathbf{W})} / |\mathbf{W}|, P_k^{(b)} \right)$$

$$v_{k|k}^{(b, \mathbf{W})} = v_k^{(b)} + |\mathbf{W}| - 1, \quad V_{k|k}^{(b, \mathbf{W})} = V_k^{(b)} + Z_k^{(b, \mathbf{W})}$$

Detected previously existing objects:

$$\alpha_{k|k}^{(j, \mathbf{W})} = \alpha_{k|k-1}^{(j)} + |\mathbf{W}|, \quad \beta_{k|k}^{(j, \mathbf{W})} = \beta_{k|k-1}^{(j)} + 1$$

$$m_{k|k}^{n, (j, \mathbf{W})} = m_{k|k-1}^{n, (j)} + K_{k|k-1}^{(j, \mathbf{W})} \varepsilon_{k|k-1}^{(j, \mathbf{W})}, \quad P_{k|k}^{n, (j, \mathbf{W})} = P_{k|k-1}^{n, (j)} - K_{k|k-1}^{(j, \mathbf{W})} \dot{H} P_{k|k-1}^{n, (j)}$$

$$v_{k|k}^{n, (j, \mathbf{W})} = \begin{bmatrix} v_{k|k-1}^{n-1, (j)} & v_{k|k}^{(j, \mathbf{W})} \end{bmatrix}$$

$$V_{k|k}^{n, (j, \mathbf{W})} = \begin{bmatrix} V_{k|k-1}^{n-1, (j)} & V_{k|k}^{(j, \mathbf{W})} \end{bmatrix}$$

$$v_{k|k}^{(j, \mathbf{W})} = v_{k|k-1}^{(j)} + |\mathbf{W}|, \quad V_{k|k}^{(j, \mathbf{W})} = V_{k|k-1}^{(j)} + \hat{N}_{k|k-1}^{(j, \mathbf{W})} + \hat{Z}_{k|k-1}^{(j, \mathbf{W})}$$

$$\hat{X}_{k|k-1}^{(j)} = V_{k|k-1}^{(j)} \left(v_{k|k-1}^{(j)} - 2d - 2 \right)^{-1}$$

$$\hat{R}_{k|k-1}^{(j, \mathbf{W})} = \rho \hat{X}_{k|k-1}^{(j)} + R \left(\dot{H} m_{k|k-1}^{n, (j)} \right)$$

$$N_{k|k-1}^{(j, \mathbf{W})} = \varepsilon_{k|k-1}^{(j, \mathbf{W})} \left(\varepsilon_{k|k-1}^{(j, \mathbf{W})} \right)^\top, \quad \varepsilon_{k|k-1}^{(j, \mathbf{W})} = \bar{\mathbf{z}}_k^{(j, \mathbf{W})} - \dot{H} m_{k|k-1}^{n, (j)}$$

$$S_{k|k-1}^{(j, \mathbf{W})} = \dot{H} P_{k|k-1}^{n, (j)} \dot{H}^\top + \frac{\hat{R}_{k|k-1}^{(j, \mathbf{W})}}{|\mathbf{W}|}$$

$$K_{k|k-1}^{(j, \mathbf{W})} = P_{k|k-1}^{n, (j)} \dot{H}^\top \left(S_{k|k-1}^{(j, \mathbf{W})} \right)^{-1}$$

$$\hat{Z}_{k|k-1}^{(j, \mathbf{W})} = \left(\hat{X}_{k|k-1}^{(j)} \right)^{1/2} \left(\hat{R}_{k|k-1}^{(j, \mathbf{W})} \right)^{-1/2} Z_k^{(b, \mathbf{W})} \left(\hat{R}_{k|k-1}^{(j, \mathbf{W})} \right)^{-\top/2} \left(\hat{X}_{k|k-1}^{(j)} \right)^{\top/2}$$

$$\hat{N}_{k|k-1}^{(j, \mathbf{W})} = \left(\hat{X}_{k|k-1}^{(j)} \right)^{1/2} \left(S_{k|k-1}^{(j, \mathbf{W})} \right)^{-1/2} N_{k|k-1}^{(j, \mathbf{W})} \left(S_{k|k-1}^{(j, \mathbf{W})} \right)^{-\top/2} \left(\hat{X}_{k|k-1}^{(j)} \right)^{\top/2}$$

$$\dot{H} = [0_{1, n-1}, \quad 1] \otimes H$$

Weights:

$$w_{k|k}^{(b, \mathbf{W})} = \frac{\omega_{\mathcal{P}} \mathcal{L}_k^{(b, \mathbf{W})} w_k^{(b)}}{d_{\mathbf{W}} \beta_{FA, k}^{|\mathbf{W}|} V(\mathcal{A})}, \quad w_{k|k}^{(j, \mathbf{W})} = \frac{\omega_{\mathcal{P}} P_D \mathcal{L}_k^{(j, \mathbf{W})} w_{k|k-1}^{(j)}}{d_{\mathbf{W}} \beta_{FA, k}^{|\mathbf{W}|}}$$

$$d_{\mathbf{W}} = \delta_{|\mathbf{W}|, 1} + \frac{\mathcal{L}_k^{(b, \mathbf{W})} w_k^{(b)}}{\beta_{FA, k}^{|\mathbf{W}|} V(\mathcal{A})} + \sum_{j=1}^{J_{k|k-1}} \frac{P_D \mathcal{L}_k^{(j, \mathbf{W})} w_{k|k-1}^{(j)}}{\beta_{FA, k}^{|\mathbf{W}|}}, \quad \omega_{\mathcal{P}} = \frac{\prod_{\mathbf{W} \in \mathcal{P}} d_{\mathbf{W}}}{\sum_{\mathcal{P}'} \mathcal{L}_{\mathbf{Z}_k} \prod_{\mathbf{W}' \in \mathcal{P}'} d_{\mathbf{W}'}}$$

$$\mathcal{L}_k^{(b, \mathbf{W})} = \frac{|\mathbf{W}|^{-d/2}}{\pi^{|\mathbf{W}|(d-1)/2}} \frac{\Gamma_d \left(\frac{v_k^{(b, \mathbf{W})}}{2} \right) \left| V_k^{(b)} \right|^{\frac{v_k^{(b)} - d - 1}{2}}}{\Gamma_d \left(\frac{v_k^{(b)}}{2} \right) \left| V_{k|k}^{(b, \mathbf{W})} \right|^{\frac{v_{k|k}^{(b, \mathbf{W})} - d - 1}{2}}} \frac{\Gamma \left(\alpha_{k|k}^{(b, |\mathbf{W}|)} \right) \left(\beta_k^{(b)} \right)^{\alpha_k^{(b)}}}{\Gamma \left(\alpha_k^{(b)} \right) \left(\beta_{k|k}^{(b, \mathbf{W})} \right)^{\alpha_{k|k}^{(b, |\mathbf{W}|)}}}$$

$$\mathcal{L}_k^{(j, \mathbf{W})} = \frac{(2\pi)^{\frac{|\mathbf{W}|d}{2}} 2^{\frac{|\mathbf{W}|}{2}}}{|\mathbf{W}|^{\frac{d}{2}}} \frac{\left| V_{k|k-1}^{(j)} \right|^{\frac{v_{k|k-1}^{(j)}}{2}}}{\left| V_{k|k}^{(j, \mathbf{W})} \right|^{\frac{v_{k|k}^{(j, \mathbf{W})}}{2}}} \frac{\Gamma_d \left(\frac{v_{k|k}^{(j, \mathbf{W})}}{2} \right)}{\Gamma_d \left(\frac{v_{k|k-1}^{(j)}}{2} \right)} \frac{\left| \hat{X}_{k|k-1}^{(j)} \right|^{\frac{|\mathbf{W}|}{2}}}{\left| \hat{R}_{k|k-1}^{(j, \mathbf{W})} \right|^{\frac{|\mathbf{W}|-1}{2}} \left| S_{k|k-1}^{(j, \mathbf{W})} \right|^{\frac{1}{2}}}}$$

$$\times \frac{\Gamma \left(\alpha_{k|k}^{(j, |\mathbf{W}|)} \right) \left(\beta_{k|k-1}^{(j)} \right)^{\alpha_{k|k-1}^{(j)}}}{\Gamma \left(\alpha_{k|k-1}^{(j)} \right) \left(\beta_{k|k}^{(j, \mathbf{W})} \right)^{\alpha_{k|k}^{(j, |\mathbf{W}|)}}}$$

IV. TRAJECTORY EXTRACTION

All components that have higher weight than a threshold \bar{w} are extracted from the PHD as targets. Note that time indexes are omitted. The extracted parameters for a component with index j are:

- The estimated trajectories over the mean and covariance of the kinematic state $m^{(j)}$ and $P^{(j)}$
- The estimated trajectory of the extension $\hat{X}^{(j)} = V^{(j)} \left(v^{(j)} - 2d - 2 \right)^{-1}$

V. EXTENSION SMOOTHING

TABLE III: Equations for the GGIWTPHD filter backwards smoothing using information from future time steps $K > k$ to improve the extension estimate at time k .

$$\begin{aligned}
 v_{k|K} &= v_{k|k} + \eta_2^{-1} \left(g - \frac{2(d+1)^2}{h+d+1} \right), \quad V_{k|K} = V_{k|k} + \eta_3^{-1} C_4 \\
 W &= V_{k+1|K} - V_{k+1|k} \\
 w &= v_{k+1|K} - v_{k+1|k}, \quad g = \eta_1^{-1} \left(w - \frac{2(d+1)^2}{n} \right) \\
 h &= \frac{d+1}{d} \text{Tr} \left\{ C_3 C_4 (C_3 C_4 - \mathbf{I}_d)^{-1} \right\} \\
 \eta_1 &= 1 + \frac{w - 3(d+1)}{n} \\
 \eta_2 &= 1 + \frac{g - 3d + 1}{h + d + 1}, \quad \eta_3 = 1 + \frac{g - d - 1}{h - d - 1} \\
 C_3 &= \mathbb{E}_{k|K} \left[\left(M_{\mathbf{x}}^{-1} W (M_{\mathbf{x}}^{-1})^\top \right)^{-1} \right] = \mathbb{E}_{k|K} \left[M_{\mathbf{x}}^\top W^{-1} M_{\mathbf{x}} \right] \\
 C_4 &= \mathbb{E}_{k|K} \left[M_{\mathbf{x}}^{-1} W (M_{\mathbf{x}}^{-1})^\top \right] = \mathbb{E}_{k|K} \left[\left(M_{\mathbf{x}}^\top W^{-1} M_{\mathbf{x}} \right)^{-1} \right]
 \end{aligned}$$

VI. MIXTURE REDUCTION

TABLE IV: Pseudocode for GGIWTPHD filter pruning, absorption and capping

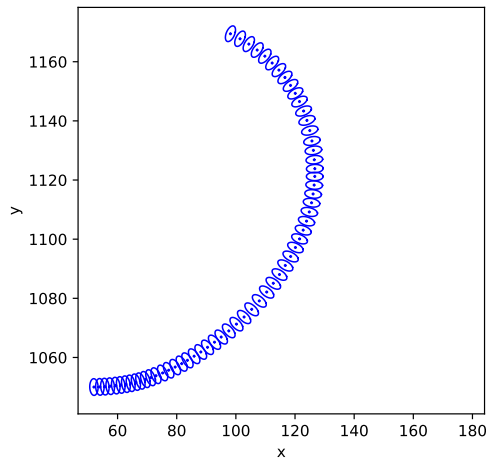
```

1: input: GGIWT components  $\left\{ w_{k|k}^{(j)}, \mathcal{T}_{k|k}^{(j)} \right\}_{j=1}^{J_{k|k}}$ , a pruning threshold  $T$ , an absorption threshold  $U$  and a maximum number of allowed components  $M$ .
2: init: Set  $\ell \leftarrow 0$  and  $I \leftarrow \left\{ i = 1, \dots, J_{k|k} \mid w_{k|k}^{(i)} > T \wedge \frac{\alpha_{k|k}^{(i)}}{\beta_{k|k}^{(i)}} > 1 \right\}$ 
3: repeat
4:    $\ell \leftarrow \ell + 1$ 
5:    $j \leftarrow \arg \max_{i \in I} w_{k|k}^{(i)}$ 
6:    $L \leftarrow \left\{ i \in I \mid \left( m_{k|k}^{n,(i)} - m_{k|k}^{n,(j)} \right)^\top \left( P_{k|k}^{n,(j)} \right)^{-1} \left( m_{k|k}^{n,(i)} - m_{k|k}^{n,(j)} \right) \leq U \right\}$ 
7:    $\tilde{w}_{k|k}^{(\ell)} \leftarrow \sum_{i \in L} w_{k|k}^{(i)}$ 
8:    $\tilde{\mathcal{T}}_{k|k}^{(\ell)} = \mathcal{T}_{k|k}^{(j)}$ 
9:    $I \leftarrow I \setminus L$ 
10: until  $I = \emptyset$ 
11: If  $\ell > M$  then replace  $\left\{ \tilde{w}_{k|k}^{(j)}, \tilde{\alpha}_{k|k}^{(j)}, \tilde{\beta}_{k|k}^{(j)}, \tilde{m}_{k|k}^{n,(j)}, \tilde{P}_{k|k}^{n,(j)}, \tilde{v}_{k|k}^{n,(j)}, \tilde{V}_{k|k}^{n,(j)} \right\}_{j=1}^{\ell}$  by those of the  $M$  components with largest weights.
12: output:  $\left\{ \tilde{w}_{k|k}^{(j)}, \tilde{\mathcal{T}}_{k|k}^{(j)} \right\}_{j=1}^{\ell}$ ,  $\tilde{\mathcal{T}}_{k|k}^{(j)} = \left( \tilde{\alpha}_{k|k}^{(j)}, \tilde{\beta}_{k|k}^{(j)}, \tilde{m}_{k|k}^{n,(j)}, \tilde{P}_{k|k}^{n,(j)}, \tilde{v}_{k|k}^{n,(j)}, \tilde{V}_{k|k}^{n,(j)} \right)$ 

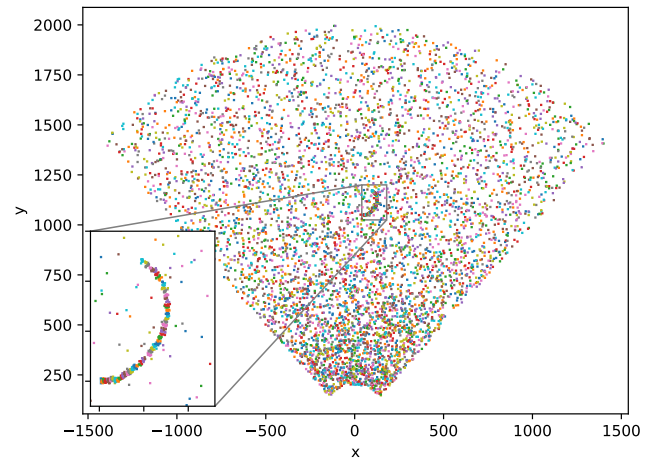
```

VII. RESULTS

A. Scenario 1

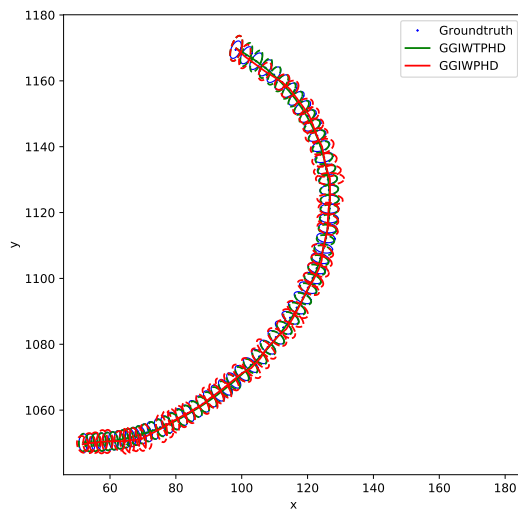


(a) Ground truth positions and extents

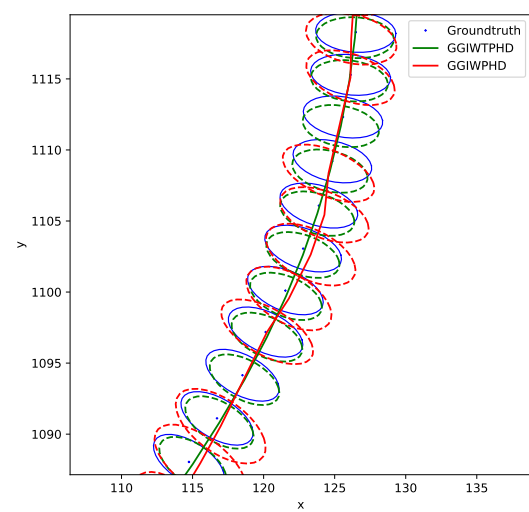


(b) Generated measurements. Note that the figure depicts all measurements over all time steps.

Fig. VII.1: Generated data used for scenario 1. One target is born at time $k = 0$ and dies at $k = 60$. It is born in the lower left and moves in a curved trajectory.

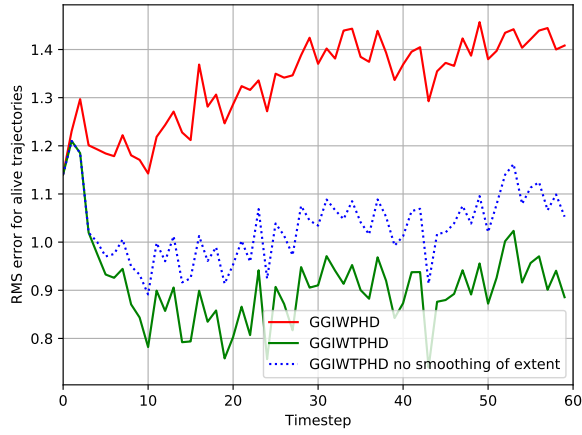


(a) Full trajectory.

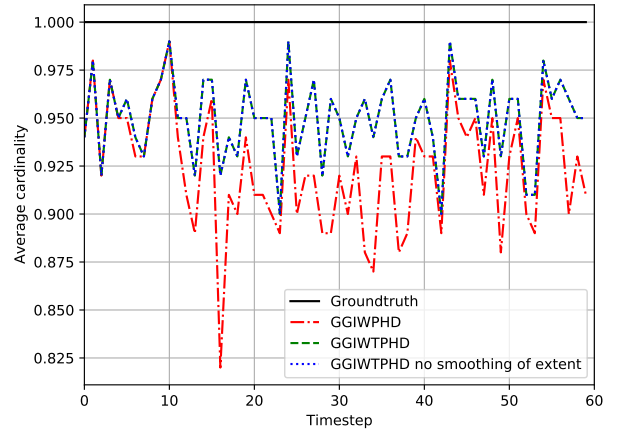


(b) Section of the full trajectory.

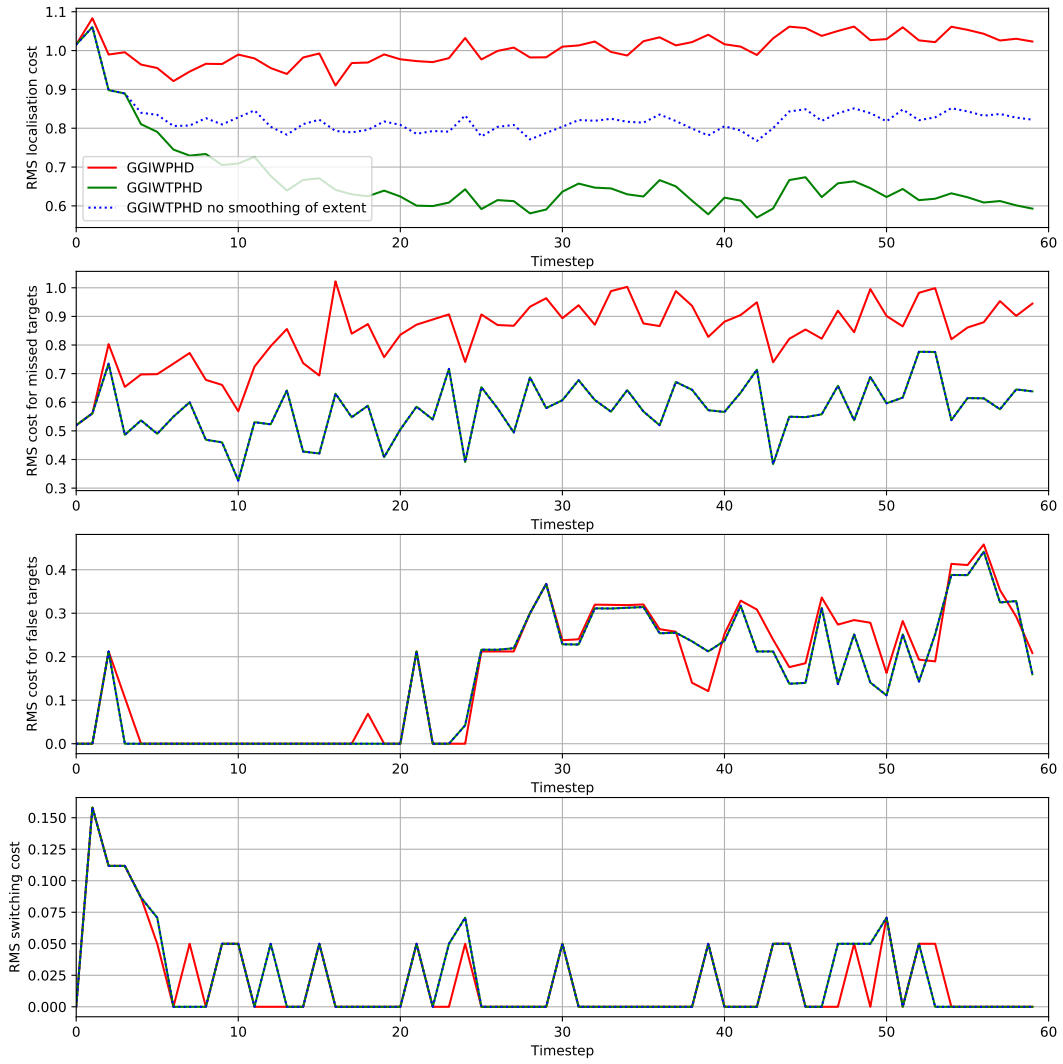
Fig. VII.2: Example of the final trajectory estimates from running both filters in scenario 1. Ground truth position and extent is given by the blue dots and ellipses. Final trajectory estimates at the end of the sequence given by the full lines for trajectories and dashed lines for the extent.



(a) RMS error of the trajectory metric



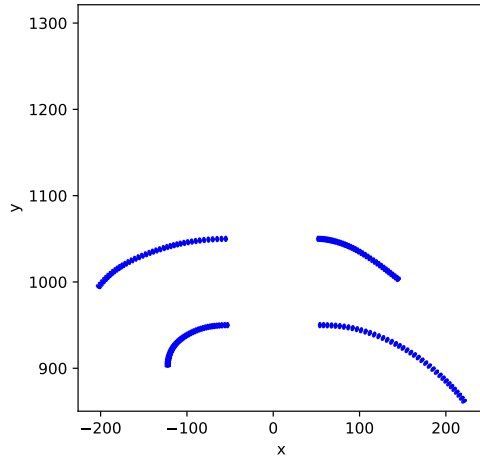
(b) Average cardinality



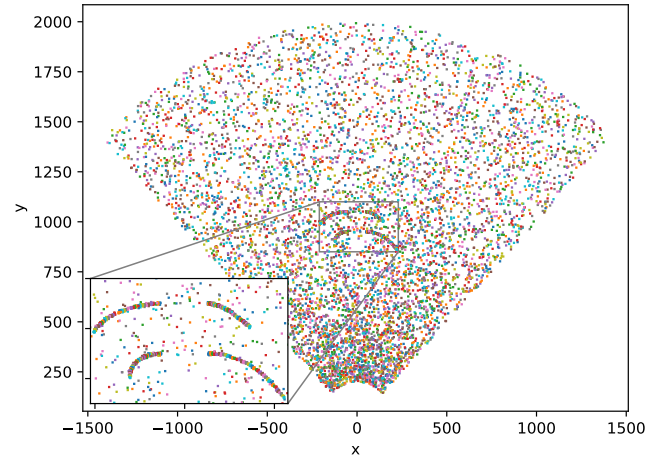
(c) Decomposed RMS costs

Fig. VII.3: Results comparing GGIWTPHD with smoothing of extent estimates, GGIWTPHD without smoothing of extent estimates and GGIWPHD using labeled components. These are results from a Monte Carlo simulation in scenario 1 of 100 runs.

B. Scenario 2



(a) Ground truth positions and extents



(b) Generated measurements. Note that the figure depicts all measurements over all time steps.

Fig. VII.4: Generated data used for scenario 2. Four targets are born at $k = [0, 10, 20, 30]$ and die at $k = [40, 50, 60, 70]$ respectively. The first is born at the top right, the second at the bottom left, the third at the top left and the fourth at the bottom right. All targets are born towards the center and move outward.

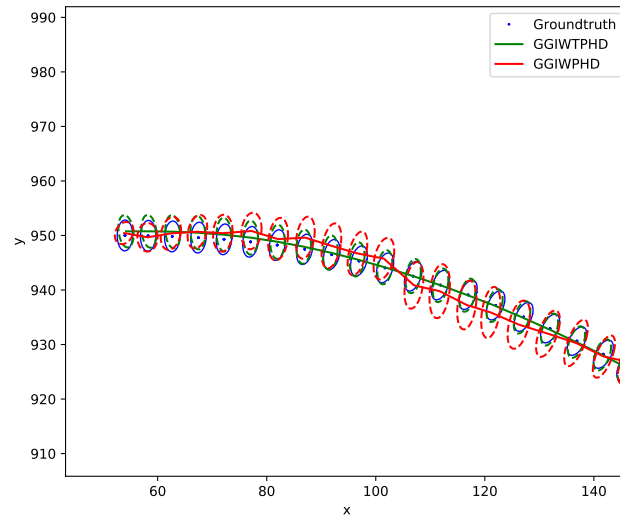
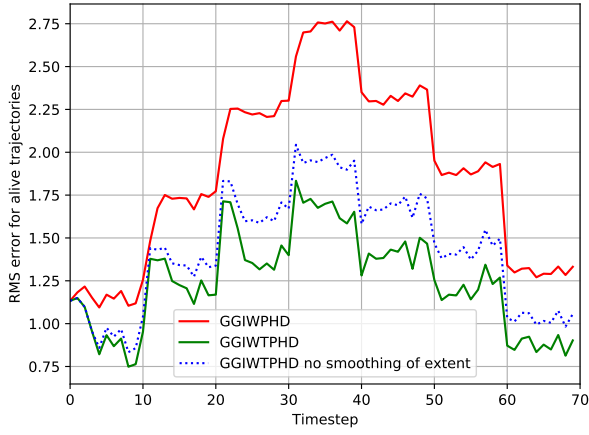
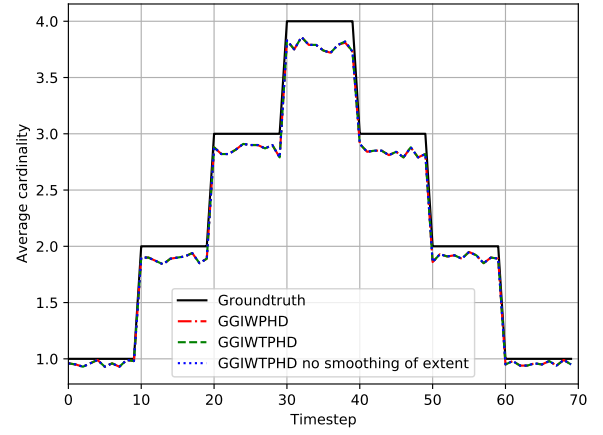


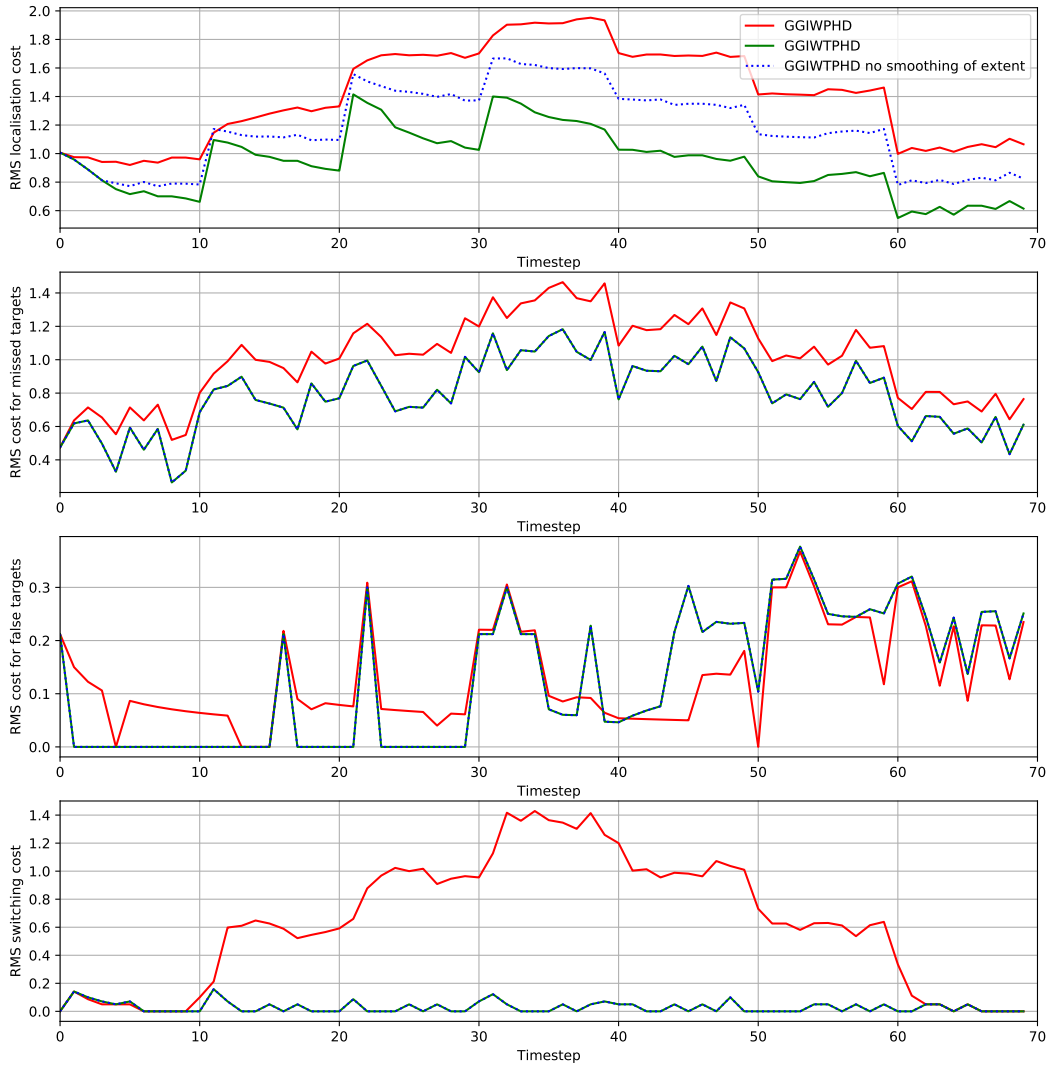
Fig. VII.5: Estimates from the start of the lower right trajectory. Ground truth position and extent is given by blue dots and ellipses. Trajectory estimates are given by the full lines for trajectories and dashed lines for the extent.



(a) RMS error of the trajectory metric



(b) Average cardinality



(c) Decomposed RMS costs

Fig. VII.6: Results comparing GGIWTPHD with smoothing of extent estimates, GGIWTPHD without smoothing of extent estimates and GGIWPHD using labeled components. These are results from a Monte Carlo simulation in scenario 2 of 100 runs.

REFERENCES

- [1] K. Granström and J. Bramstång, "Bayesian Smoothing for the Extended Object Random Matrix Model," *IEEE Trans. Signal Process.*, pp. 3732–3742, 2019.
- [2] K. Granström and U. Orguner, "Estimation and maintenance of measurement rates for multiple extended target tracking," in *2012 15th International Conference on Information Fusion*, Singapore: IEEE, 2012, pp. 2170–2176.
- [3] K. Granström, A. Natale, P. Braca, G. Ludeno, and F. Serafino, "Gamma Gaussian Inverse Wishart Probability Hypothesis Density for Extended Target Tracking Using X-Band Marine Radar Data," *IEEE Trans. Geosci. Remote Sens.*, pp. 6617–6631, 2015.